Department of Physics

STATE UNIVERSITY OF IOWA

Iowa City

DIRECT DETERMINATION OF PRIMARY COSMIC RAY ALPHA PARTICLE ENERGY SPECTRUM BY NEW METHOD*

by

Frank B. McDonald

Department of Physics
State University of Iowa
Iowa City, Iowa

March 1956

*Assisted by Joint Program of Office of Naval Research and Atomic Energy Commission.

ERRATA

1. Page 1, Line 19 - Read "response" instead of "respons".
2. Page 2, Line 7 - Delete the comma after Z.
3. Page 4, Line 14 - N_c; c is lower case.
4. Page 5, Line 12 - Delete comma after Cerenkov.
5. Page 6, Line 8 - Should read $\lambda = 55^{\circ}N$.
6. Page 8, Line 22 - Read "three" instead of "these".
7. Page 15, Line 10 - Insert "is" after "this".
8. Page 19, Line 15 - Change "or" to "of".
9. Page 23, Line 13 - Read "energy" instead of "enerby".
10. Page 25, Line 2 - Change "alpha" to "alphas".
11. Page 30, Line 7 - Read "monatomically" instead of "monaomically".
12. Page 34, Line 24 - Change $J(= E)$ to $J(\geqq E)$.

ABSTRACT

The flux of cosmic ray alpha particles has been measured at $\lambda = 41^{\circ}N$ and $55^{\circ}N$ and the energy spectrum in the region 883-285 Mev/nucleon has been determined by the use of a combination of a scintillation counter and Cerenkov counter. This spectrum is not dependent on geomagnetic theory. It has been found that the integral alpha spectrum can be fitted with the function

$$J_{O_\alpha}(E) = \frac{435}{(1+E)^{1.4 \pm .2}} \text{ Particles } /M^2\text{-sec-ster}$$

and

$$J_{O_\alpha}(E_1) = 88 \pm 9 \text{ Particles } /M^2\text{-sec-ster } \lambda = 41^{\circ}N.$$

$$J_{O_\alpha}(0.285 \text{ Bev}) = 292 \pm 25 \text{ Particles } /M^2\text{-sec-ster } \lambda = 55^{\circ}N.$$

$J_{O_\alpha}(E)$ is the flux of α particles at the top of the atmosphere with kinetic energy $\geq E$ (in Bev/Nucleon). E_1 is the cut off energy/nucleon for α particles at $41^{\circ}N$. An absorption mean free path $\lambda_\alpha = 45 \pm 7$ g/cm^2 has been measured for alpha particles. The properties of this new detector are discussed and a study is made of the energy respons of the Cerenkov counter to fast multiply charged particles.

I

Introduction

Recently it has been demonstrated 1,2,3 that it

1. J. Linsley, Phys. Rev. 97, 1292 (1955).
2. N. Horowitz, Phys. Rev. 98, 165 (1955).
3. W. R. Webber and F. B. McDonald, Phys, Rev. 100, 1460 (1955).

is possible to obtain consistent and accurate flux values of the low Z, components of the primary cosmic radiation by using Cerenkov counters at low latitudes. These experiments have provided excellent charge resolution for Z = 1, 2 and adequate resolution in the Z = 3 - 8 range. However, it appears impossible to extend these measurements to higher latitudes since, with the Cerenkov counter, slow high Z particles give pulses equivalent to those of fast particles of lower charge. If such an extension were possible it would be of great interest since the region from 41° to 55° geomagnetic latitude covers the velocity sensitive region of the average Cerenkov counter, and it should make possible the direct determination of the energy spectrum of various components without having the uncertainties introduced by combining the geomagnetic theroy with a latitude survey. In addition, an electronic detector has great advantages

Hill, 1949).

It will be noted that for the Cerenkov detector the output signal, Nc, is decreased as the velocity is decreased, while for the ionization detector the output signal is increased as the velocity is decreased. In Figure 1, a plot is given of the response of such a combination of these two types of detectors to protons and alpha particles in the energy range above 320 Mev/Nucleon. The ordinate gives the most probable output signal from the Cerenkov counter for a particle of charge Z and energy E, while the abscissa gives the corresponding most probable energy loss $\mathcal{E}_p$ in the ionization device. For energies less than 1 Bev/Nucleon, the curve of $\mathcal{E}_p$ vs N_c can be represented by:

$$N_c = Z^2 K_1 - K_2 \mathcal{E}_p \qquad (3)$$

where K_1 and K_2 are constants.

With the individual detectors, resolution of the cosmic ray charge spectrum is possible only for relativistic particles. However, Fig. 1 demonstrates that the combination of these two types of detectors gives charge resolution which is independent of velocity. This resolution will be extended below the Cerenkov threshold due to material in the telescope beneath the ionization detector. In the present experiment incident particles

must have an energy greater than 120 Mev/Nucleon. This prevents slow protons from extending into the non-relativistic alpha region. Since the response of both detectors is velocity dependent, it follows that if effective charge resolution can be achieved, it will also be possible to obtain a velocity spectrum of the various Z components of the cosmic radiation in the range of 1 Bev to 100 Mev. This determination of the energy spectrum would depend only on the properties of the detector and would be independent of geomagnetic theory. In addition other useful information would be obtained. Because of the directional properties of the Cerenkov, counter particles lying along the line A-B in Fig. 1 would represent the upward moving albedo of the cosmic radiation, and it would be possible to gain some idea of the energy distribution of these particles. The particles lying along R-B where R is at the vertical geomagnetic cut-off energy would represent most of the protons in the returning albedo and slow secondaries generated in the atmosphere.

Detectors using this principle have been developed at the State University of Iowa, and three flights using Skyhook balloons have been completed. Two flights were made at $\lambda = 41^{\circ}N$ (San Angelo, Texas) to test the response to fast particles and to note whether there was any

background in the multiply charged, low energy particle region. It was observed that while the charge resolution was comparable to, or better than, that obtained by using the Cerenkov counter at the same latitude, it still did not represent an optimum response. The resolution was further improved by better selection of photomultipliers and by reducing the amount of material in the telescope. One flight was made at $\lambda = 55^{\circ}N$ (Minneapolis, Minn.) on 7 July 1955. These initial flights were made to measure the proton and alpha particle flux. Further flights are planned at 58°, 55° and 52° to study Z = 1 - 6 components. It is the results of the flight at $\lambda = 55^{\circ}N$ dealing with alpha particles, in addition to related data from the $\lambda = 41^{\circ}N$ flights, that will be discussed in this paper. The data on primary protons and cosmic ray albedo will be discussed in a future paper.

II

Apparatus

A schematic drawing of the telescope is given in Figure 2. A scintillation counter using a Na - I (Th. act.) crystal was used for the ionization detector. Lucite was selected for the Cerenkov radiation because its index of refraction is convenient in the energy range of greater than 320 Mev/nucleon. The bottom telescopic element is a 15.24 cm. x 14.7 cm. array of Geiger counters. The counters have an effective length of 14.7 ± 0.3 cm.. The wall thickness is 0.088 mm. copper. The telescope geometric factor is 4.02 ± 0.15 $cm.^2$-ster for Flight III and $7.25 \pm .3$ cm^2-ster for Flight I.

Fig. 3 gives a schematic drawing of the electronic circuits. The arrangement is a modification of the design used by Ney and Thon[6] on the first Skyhook

---

6. E. P. Ney and D. M. Thon, Phys. Rev. 81, 1068 (1951).

---

scintillation counter flight. The signals from the two detectors are amplified by linear amplifiers and displayed on the vertical plates of two cathode ray tubes. A coincidence is formed when there is a simultaneous pulse from the Geiger counter tray and a pulse greater

than .5 x the most probable energy loss for a proton at minimum ionization in the crystal channel. The coincidence pulse operates an intensifier circuit and the pulses from the two scopes are recorded by an open shutter camera with continuously moving film. It will be noted that this is just the familiar technique of using the cathode ray tubes as master coincidence elements. The pulses from the lower geiger counter tray also actuate a shower circuit so that there is an indication on the horizontal CRT plates when an event occurs and more than one counter in the lower tray is discharged. A ring of guard counters is placed above the lower tray to assist in the detection of stars and side showers and to provide better definition of the telescope geometric factor. These counters also give deflections on the horizontal plates when any one of the four is discharged. The action of the multiple particle detectors is to give the pulses an inverted "J" appearance and these pulses will be referred to as J pulses in contradistinction to the normal pulses arising from the passage of a single particle through all these elements of the telescope. For flights the complete assembly with the necessary battery packs is placed in a thin aluminum pressurized container. Pressure-altitude data is obtained by photographing a model FA160 Wallace and Tiernan gauge in an independent unit.

III

Detector Resolution

The sea level cosmic ray mu mesons are convenient particles for checking the resolution of the telescope. In actual practice, particles of a given charge will not lie along one of the lines shown in Figure 1, but will be distributed in a region about this line due to various types of fluctuations. In the scintillation counter the principal fluctuation is the Williams-Landau effect. This fluctuation arises when fast charged particles traverse a thin absorber since large energy transfers to single electrons can occasionally occur. The most probable energy loss, ϵ_p, is given by Formula 1 and there is a straggling of the individual losses around this value. The fluctuations in energy loss were first calculated by E. J. Williams[7] and later more accurately in closed form by Landau[8] and by Symon[4]. The curves presented

---

7. E. J. Williams, Proc. Ruy, Soc. A125, 420 (1929).
8. L. Landau, Journal of Physics USSR 8, 201, (1944).

in Symon's thesis are used in the calculation on fluctuations in energy loss. Fig. 4 gives an observed pulse height distribution for sea level mu mesons and the predicted curve based on the Williams-Landau effect. It is seen that excellent agreement with the predicted curve is obtained on the high energy side of the curve. The effect of electrons escaping from the crystal is partially offset by the presence of 1.5 g/cm^2 of glass and Al above the crystal. In the calculated curve a mean meson energy of 1 Bev is assumed. The actual mu meson energy spectrum introduces a negligible error in the calculation. The additional broadening of the distribution is due primarily to non-uniformity of light collection with a much smaller contribution from photon statistics. In Figure 5 is shown the calculated Williams-Landau distribution for α particles with energies of 4, 1.5, .8, .4, .3 and .2 Bev/nucleon. The distributions become more gaussian in shape and become progressively sharper as the kinetic energy of the particles is decreased. A fortunate circumstance occurs in that the fast α particles ($E > 1.5$ Bev. nucleon) and sea level mu mesons will both have approximately similarly shaped distributions in the ionization detector. This arises because the two major sources of fluctuation - the Williams-Landau effect and the non-uniformity of light collection - are the same for both.

The fractional spread of the Williams-Landau distribution is a very slowly varying function of $\mathcal{E}_p$ for fast particles when $E/m_o c^2 > 2$ and $E >> \mathcal{E}_p$. A comparison of the sea level mu mesons distribution, shifted to the α-region, and primary cosmic ray primary alpha particle distribution obtained on Flight #I, January 1955 at $\lambda = 41^o$ is given in Figure 6. As will be apparent later, the major correction for the raw data involves the high energy tail on the fast particle distributions. The close agreement between the predicted distribution and the experimental distribution as shown in Fig. 4 and 6 gives increased confidence that this correction can be applied with a high degree of accuracy.

In the Cerenkov counter the major source of fluctuations is due to photon statistics. While the number of useable photons produced by the passage of a fast singly charged particle through the lucite is of the order of 1200, the photoelectric efficiency of the photocathode surface is low and the actual number of photoelectrons will be of the order of 40 resulting in an approximate Poisson distribution. Fig. 7 gives the experimental Cerenkov distribution for sea level mu mesons. The dotted line represents the Poisson distribution for $\bar{n} = 34$. Since part of the broadening

of the distribution is due to cascading stages, each having a Poisson distribution, the actual number of photoelectrons will be greater than $\bar{n} = 34$ and will depend on the secondary emission ration of the various stages and focusing losses between dynodes. It is seen in Figure 6 that the observed distribution is asymmetric . This represents an effect in the Cerenkov counter similar to the Williams-Landau effect in an ionization detector.

IV

FLIGHT DATA

The time-altitude data for Flight I at $\lambda = 41°$ (San Angelo, Texas) on 17 Jan. 1955 and Flight III at $\lambda = 55°$ (Minneapolis, Minn.) on 7 July 1955 are given in Figure 8. The time in each case is central standard time. The accuracy of pressure determination is better than .5mb. The agreement with the telemetered data furnished by the balloon contractor, Winzen Research, Inc. of Minneapolis, Minnesota was generally within 1 mb.

In both flights the equipment was recovered in operating condition and immediate tests were carried out to insure that the apparatus was functioning properly and in particular that the geiger counter plateaus had not shifted. In each case there was no discernible shift in any component.

Reeuction of the data was carried out by displaying the film on a Model C Recordax microfilm reader and, for each event, measuring the pulse height in the Cerenkov channel and in the ionization channel. It was also noted whether one of the multiple event detectors had been actuated for a given event. Appropriate time intervals were selected, with a maximum interval of 20 minutes being used. The data were tabulated on a 40×40 rectangular array. On the film, the average

spacing between counts is not large and care is required to insure that the proper pair of pulses is selected. In less than 1% of the counts, it was not possible to make an effective separation between a pair of events.

After the film data had been transferred to the 40 x 40 array, it became obvious that due to the widths of the distributions, it would not be possible to use equation 3 in obtaining the flux values. It was then decided to divide the data into various ionization intervals and study the Cerenkov distributions in these intervals. This is illustrated in the corrected data of the α particle region given in Fig. 9. These give the distribution of the regular Cervenkov counts in the selected ionization intervals. The same data, along with the distribution of the "J" counts are given in Fig. 10. No corrections have been applied. The ionization intervals chosen correspond to kinetic energies per nucleon at the top of the atmosphere of >1.5 Bev., $>.883$ Bev., .570-.883 Bev., .436- .630 Bev., .320 - .436 and .286 - .361 Bev.. The intervals were selected so that there were, to a crude approximation, equal numbers of alpha particles in each of the intervals which were in the energy sensitive region (i.e., $E < 900$ Mev/nuc). Certain features of the curves are immediately apparent. One notes in the fast particle region the excellent peak to valley ratio,

and the manner in which the curves go to zero on the high side of the distribution. It is also seen in Fig. 10 that the J distribution is slightly peaked under the alpha region and that most of these counts can be accounted for by δ rays and interactions in material in the telescope below the Cerenkov detector. It is felt that the good peak to valley ratio, the sharp fall-off on the high side of the distribution and the "J" pulse distribution indicate a minimum of background in the alpha region. This further strengthened by the observed altitude dependence given in Fig. 11 which will be discussed later.

CORRECTIONS IN ALPHA REGION

There are four corrections to be applied to the observed alpha data in order to deduce an absolute flux at the top of the atmosphere. There are: a general background correction, a correction for the absorption of alpha particles in the telescope and in the atmosphere above the telescope due to nuclear interactions, a δ ray correction, and a correction for the production of alphas in the atmosphere by the fragmentation of primary heavy nuclei.

The shape of the background correction is taken to be the interval at $3x\mathcal{E}_p$ for protons at minimum ionization. In Fig. 1 this corresponds to a line drawn parallel to the ordinate and intersecting the abscissa at 3.6 on the arbitrary scale. The ionization distribution rises rapidly so it is possible to select a region just behind a group of particles with the desired charge and this region will be almost completely free of particles with this charge. The flight at $\lambda = 41^0$N demonstrates that the shape of the background curve did not change across the complete alpha interval. The background curve obtained at $\lambda = 55^0$N was normalized on the low energy side of the Cerenkov distributions. The corrections to the various intervals by this method are given in Fig. 10.

In order to correct for the attenuation of the alpha particles by nuclear interactions it is necessary to know the interaction mean free path, λ_α. There are several experimental determinations of λ_α. Waddington[10] has used emulsion at $\lambda = 55^0$, Webber

10. C. J. Waddington, Phil Mag. 45, 1312 (1954).

and McDonald[3] at $\lambda = 41^0$ observed the atmospheric attenuation as detected by a Cerenkov counter and Quarenti and Zorn[11] used 90 Mev/ nucleon alpha

11. G. T. Quarenti and G. T. Zorn, Nuovo Cimento 1, 1282 (1955).

particles from the Berkley cyclotron. All values obtained are in good agreement with the semi-empirical relation proposed by Bradt and Peters[12]:

12. Bradt and Peters Phys. Rev. 77, 54 (1950).

$$\sigma = \pi(r_1 + r_2 - 2\Delta r)^2$$
$$r_i = 1.45 \times 10^{-13} A_i^{\frac{1}{3}} \text{ cm.}$$
$$\Delta r = .85 \times 10^{-13} \text{ cm.} \qquad (4)$$

A_1 = mass number of incident nuclei

A_2 = mass number of target nuclei

σ = interaction cross section

This gives a value of λ_{α}(air) = 44 g/cm^2. The observed atmospheric absorption of α's in this experiment is given in Fig. 11. This gives a value of λ_{α} =45±7g/cm^2. The work of Quarenti and Zorn at low energies gives added confidence that the collision cross section is not strongly energy dependent. A compilation of the observed values of λ_{α} for the various experiments is given in Table I. The nuclear interaction correction factor for Flights I and III is summed up in Table II.

The δ ray correction is necessary as it is possible for particles traversing the top two elements of the telescope to produce knock-on electrons which will trigger one of the geiger counters. For particles which would normally pass through the telescope, this results in their being classified as J counts. Some particles which miss the bottom element will appear as regular counts and there will be a spurious increase of the geometric factor. Because of the straggling of the electrons in the block and in the counter walls, it is difficult to compute this correction with confidence. However an upper limit to the correction can be obtained and this upper limit probably represents a good approximation to the true correction. If one neglects straggling then the number of knock-ons, N_{δ_j}, per particle which trigger a counter in the lower tray

Table I

Observed M.F.P. of Helium Nuclei in Emulsion and Air

Investigator	Lat.°	Detector	λ_α (Exp) g/cm^2	λ_α (calc. from eq. 4) g/cm^2
Waddington[10]	55°	Emulsion	60 ± 17	72
Quarenti Zorn[11]	90 Mev/Nuc α from Berkeley cyclotron	Emulsion	80 ± 6	72
Webber McDonald[3]	41°	Cerenkov counter	43 ± 8	44
McDonald (Present Experiment)	55°	Cerenkov and Scint. Counter	45 ± 7	44

Table II

Correction for Attenuation of α's

by Nuclear Interactions

Flight	Lat.	X_1 Atmos. Depth of Detector	X_2 Amount of Material in Telescope $\bar{z} = 15$	$e^{-\left(\frac{X_1}{\lambda_{\alpha_1}} + \frac{X_2}{\lambda_{\alpha_2}}\right)}$
I	41°N	15.1 g/cm^2	9.08 g/cm^2	.580
III	55°N	12.4	9.2	.613

can be calculated. This quantity can also be determined experimentally for sea level mu-mesons, and this is designated as $(N_{\delta M})$ exp. The ratio of $(N_{\delta M})$ exp/ $(N_{\delta M})_c = \gamma$ is taken as a correction factor to be applied to $(N_{\delta\alpha})_c$. If one neglects straggling then the number of knock-ons which trigger the bottom tray is given by

$$(N_{\delta Z}) = \frac{\kappa Z^2}{\beta^2} \int_{x_1}^{x_2} \int_{\varepsilon'(x_1)}^{\varepsilon'_{max}} \left(1 - \beta^2 \frac{\varepsilon'_\delta}{\varepsilon'_{\delta max}}\right) \frac{d\varepsilon'_\delta}{\varepsilon'^2_\delta} \, dx \qquad (5)$$

The range-energy relation for electrons is given by[13]

$$E = ax + c = 1.83x + .133 \text{ Mev.}$$

and

$$E_1 = ax_1 + c = 1.25 \text{ Mev.}$$

---

13. Glendenin, L., Nucleonics 2, No. 1, 12 (1948).

In these formulas β and Z are the velocity and charge of the incident particle, x_1 is the thickness or the geiger counter wall, x_2 is the total amount of material in the telescope and E_2 is equal to 15 Mev. $E_{\delta\,max}$ is the maximum energy which can be transferred to an electron by a heavy particle of velocity β.

If $F'_{\delta\,max} \geq x_2 + C = E_2$ (this corresponds to $\sim$ 3 Bev/nuc for alpha particles) then $(N_{\delta z})_c$ reduces to

$$(N_{\delta z})_c = \frac{\kappa Z^2}{\beta^2 \alpha} \left[\left(1 + \beta^2 \frac{\varepsilon_1}{\varepsilon_{\delta max}}\right) \ln \frac{\varepsilon_{\delta max}}{\varepsilon_1} - (1+\beta^2)\left(1 - \frac{\varepsilon_1}{\varepsilon_{\delta max}}\right) \right] \qquad (6)$$

$$\text{The ratio } \frac{(N_{\delta\mu})_{exp}}{(N_{\delta\mu})_c} = \gamma = \frac{.018}{.075} = .24$$

The experimentally determined ratio γ was used to correct $(N_{\delta\alpha})_c$ at various energies. These corrections are given in Table III. It is seen that in the energy sensitive region of the detector (i.e., $E <$ 1 Bev), this correction is negligible. For the Flights at 41° the bottom ring of guard counters was omitted and the δ-ray correction was -2o/o. In this correction the δ-ray angular distribution of $\cos^{2.5}\theta$ measured by Brown, McKay and Palmatier[14]

14. W. W. Brown, A. S. McKay and E. D. Palmatier, Phys. Rev. 76, 506 (1949).

on sea level mesons was used, where θ is the angle between the δ-ray emerging from the block and the track of the particle which produced the δ-ray.

To extrapolate the observed alpha flux to the top of the atmosphere it is also necessary to correct for the production of energetic α particles by the fragmentation of heavy nuclei above the telescope.

Table III

E_{α} Kinetic Energy/ Nucleon of Incident α	$E'_{\delta\ max}$ Maximum Energy δ Ray which can be produced by alpha with energy =E	$(N_{\delta\alpha})_c$ Number of δRays/α which trigger geiger counter array (Straggling neglected)	$\gamma (N_{\delta\alpha})_c$ number of δrays/α which trigger geiger counter array with empirical straggling correction
4 Bev	28 Mev	.18	.045
2	8.75	.10	.025
1	3.29	.037	.010
.8	2.42	.017	.043
.6	1.7	.005	.001

This is similar to the correction necessary in the Li, Be and B region. Noon and Kaplon[15] have derived the

15. J. H. Noon and M. F. Kaplon, Phys. Rev. 97, 769 (1955).

fragmentation probabilities for incident medium and heavy nuclei in air based on the observed interactions in emulsion. The value for the fragmentation probability, $P_{x\alpha}$ which is the average number of alphas produced in a nuclear interaction initiated by the x^{th} component and appropriate heavy flux values are summed up in Table IV. A standard diffusion equation is used to obtain the actual number of secondary alphas incident on the telescope.

At $\lambda = 55^{o}$ number of secondary alphas at 12 g/cm^2 = 11 $\pm$ 4 particles/m^2-sec-ster.

At $\lambda = 41^{o}$ number of secondary alphas at 15 g/cm^2 = 6.5 $\pm$ 3 particles/m^2-sec-ster.

This correction has not been applied to the differential and integral spectrum in Fig. 14 and 15 and in Table 4.

Table IV

Flux Values and Fragmentation Probabilities Used in Fragmentation Correction

	J_o ($Z \geq 1^o$) Particles/ M^2/sec/ster	$P_{H\alpha}$	J_o (C-N-O-F) Particles/ M^2/sec/ster	$P_{M\alpha}$ [a]	J_o(Li,Be, B) [d]	$P_{L\alpha}$ [e]
$\lambda = 55^o$	4.2 ± 1.5 [b]	2.07 [a]	12 ± 1 [b]	1.42 [a]	$\frac{1}{2} J_o$(C-N-O-F)	.9
$\lambda = 41^o$	$2.4 \pm .3$ [c]	2.07 [a]	5.9 ± 0.7 [c]	1.42 [a]	$\frac{1}{2} J_o$(C-N-O-F)	.9

(a) See reference 15,

(b) Danton, Fowler and Kent, Phil. Mag. 43, 729 (1952).

(c) Kaplon, Peters, Raynolds and Ritson, Phys. Rev. 85, 295 (1952)

(d) Kaplon, Noon and Racette, Phys. Rev. 96, 1408 (1954)

(e) Derived from fragmentation table data of K. Gottstein, Phil Mag. 45, 347 (1954).

V

ENERGY CALIBRATION

The selected intervals of ionization were calibrated in terms of the most probable energy loss for α particles at minimum ionization, $(\mathcal{E}_p)_{\alpha\ min}$. From the data at $\lambda = 41^\circ$ it is known that some 25% of the alphas at 55° will have energies greater than 2 Bev/Nuc and will be at minimum ionization. The ionization distribution of these particles can be studied by selecting an interval along the high side of the Cerenkov distribution. In Fig.1 this corresponds to taking an interval parallel to the $\mathcal{E}_p$ axis and intersecting the Cerenkov axis at 21. This gives a pulse height distribution similar to that shown in Fig. 6. The peak in the distribution thus obtained is $(\mathcal{E}_p)_{\alpha\ min.}$ and the values of $(\mathcal{E}_p)_\alpha$ of the other intervals are known in terms of $(\mathcal{E}_p)_{\alpha\ min.}$ since the system is a linear one. The peak in the ionization distribution is quite accurately defined and the position of $(\mathcal{E}_p)_{\alpha\ min,}$ on the 40 x 40 array is known to 3%. A curve of $(\mathcal{E}_p)_\alpha$ vs. kinetic energy as calculated by Eq. 1 is given in Fig. 12. The abscissa could also have been plotted in terms of $(\mathcal{E}_p)_\alpha$ / $(\mathcal{E}_p)_{\alpha\ min.}$ since this was the quantity actually used

VI

ALPHA ENERGY SPECTRUM

To derive an energy spectrum from the distributions given in Fig. 10 it is necessary to relate the observed number of particles within an interval of energy loss to the actual number in the corresponding energy interval. The calibration of the energy intervals in terms of ionization loss was discussed in the previous section. However, due to fluctuations introduced by detectors, the number of particles within an interval of energy loss is not necessarily the number in the related energy interval. The largest correction will be the Williams-Landau correction for high energy alphas. It is a major correction only in the energy region $\geq$ 1 Bev and becomes completely negligible at energies less than .6 Bev./nuc. This is illustrated in Fig. 5. As has been discussed in Section 3 this correction can be computed quite accurately. This correction has been calculated for intervals I and II ($E >$ 883 Mev/nuc) and III (570-883 Mev/nuc.). The effect of applying this correction is to remove the asymmetry in the ionization distribution. Thus the pulse height distributions from both detectors should be approximately gaussian in the energy sensitive region. If

now the intervals have been selected so that there are equal numbers of alpha per interval after the Williams-Landau asymmetry has been removed, then this number should represent a good approximation to the actual number of particles in the energy interval since the loss to neighboring intervals will tend to be balanced by the gain from these intervals. The energy spectrum data are summarized in Table V. It is seen that this condition has been well satisfied in intervals 3 and 4 but the value of N_α falls off in intervals 5 and 6. A correction factor was computed by the synthesis of the pulse height distributions. This correction factor was never greater than 10%. This gives added confidence that this method of analysis has not introduced major errors in the derivation of the energy spectrum. In a similar manner the contributions of intervals I and II to III were computed. This is necessary because of the great difference in N_α in the 3 intervals. These corrections have all been applied with the Williams-Landau correction in column 6 of Table V. In Column 7, N_α is converted to a vertical flux value and in Column 8 the δ ray correction and the correction for nuclear absorption in the telescope and in the atmosphere above the telescope have been applied. In

Column 9 the values for the differential energy spectrum are given. The flux data for Flight I are also included in Table V. Fig. 13 and Fig. 14 give the points obtained for the differential and integral energy spectrum. In each graph the high energy point makes use of $J_{o\alpha}$ at 41°N. A geomagnetic cut-off of 1.65 Bev/Nuc has been calculated for this point. This is the only point dependent on geomagnetic theory. Also in Fig. 13 are the experimental points measured by Waddington[10] at $\lambda = 55°$ using emulsion. The general agreement is good. The data in Fig 13 and 14 have been fitted with a curve of the form

$$J_{o\alpha} (\geq E) = \frac{C}{(1+E)^{\gamma}}$$

E = kinetic energy in Bev.

It is found that a best fit is found for:

$\gamma = 1.4 \pm .2$ and $c = 431$.

The vertical flux values at $\lambda = 55° + 41°$ are

$J_{o\alpha}$ (E>285 Mev/Nuc) = 306 ± 24 particular/M^2-sec-ster (without fragmentation correction)

$J_{o\alpha}$ (E_1) = 96 ± 9 " " " " "

E_1 = vertical geomagnetic cut off in Bev/Nuc at 41°.

When the fragmentation correction is applied

$J_{o\alpha}$ (E 285 Mev/Nuc) = 292 ± 25 Particles/M^2-sec-ster

$J_{o\alpha}$ (E_1) = 88 ± 9 " " " " "

Table V

Flight III λ = 550

Interval	$\frac{dE}{dX}$ in Crystal in Mev	Energy Interval Defined at 12 gms residual Atmosphere Mev/Nuc	Energy Interval Corrected to Top, of Atmos. Mev/Nuc	N # of a counts in int.	N_α with Landau-Williams Correction	J_α at 12g/cm^2 Particles/ M^2-sec-ster/ interval	$J_{o\alpha}$ particles/ M^2-sec-ster/ interval	$\frac{dJ_{o\alpha}}{dE}$ Number of α'S/ M^2-sec-ster/ Mev
I & II	<5.68	>855	> 883	525	784	108	182	
III	5.68-6.70	540-855	570-883	348	190	26.0	42.5	136 ± .02
IV	6.45-7.75	398-600	436-630	285	202	27.8	45.5	.24 ± .03
V	7.75-9.30	278-398	320-436	166	145	20.0	32.6	.28 ± .045
VI	8.52-10.06	241-328	286-361	134	118	15.8	27.7	.37 ± .06

Flight I λ = 41°

N_α # of Alpha counts	J_α at Detector particles/ M^2-sec-ster	$J_{o\alpha}$ Particles/ M^2-sec-ster at top of atmosphere without (fragmentation correction)	$J_{o\alpha}$ Particles/ M^2-sec-ster at top of atmosphere with fragmentation correction
460 ± 22	560	96 ± 8	87 ± 9

Because of a gain shift caused by repairs just prior to launching, it was not possible to say anything concerning the geomagnetic cut-off at $\lambda = 55^{\circ}$ except that it is less than 285 Mev/Nuc.

Table VI provides a summary of α flux measurements at $\lambda = 41^{\circ}$ and 55°. The over-all agreement is quite good.

16. Perlow, Davis, Kissinger and Shipman
Phys. Rev. 88, 321 (1952).
17. J. Linsley, Phys. Rev. 101, 826, (1956)
18. L. Bohl, University of Minnesota, Thesis (1954).
19. L. R. Davis, H. M. Caulk and C. Y. Johnson
Phys. Rev. 101, 800 (1956).
20. F. B. McDonald, University of Minnesota Thesis
(1955).

Climax, Colorado. There are no observed fluctuations during the period of the flight and the neutron counting rate is in close agreement with the yearly mean - illustrating that this was a "normal cosmic ray day".

VIII

ENERGY RESPONSE OF CERENKOV COUNTER TO FAST MULTIPLY CHARGED PARTICLES

The theoretical Z and β dependence of the Cerenkov radiation is given by equation 2. However this equation was not used explicitly in deducing the energy spectrum. It was assumed merely that the N_c was Z dependent and decreased monaomically as the velocity decreased. It is of interest to measure the Z and β response of the Cerenkov counter to fast multuply charged particles. By comparing the relativistic proton and alpha distribution (E 2 Bev/Nuc) it was established that for $\beta \approx 1$, the radiation varied as Z^2 within the 7% experimental error. The β dependence of the Cerenkov radiation can be studied by noting the position of the peak in the Cerenkov distribution in the various ionization intervals given in Fig. 10. These experimental points have been normalized to the theoretical curve at interval I ($\bar{E}$ = 3 Bev.). Agreement with the theoretical curve is excellent for the higher values of E. However at levels near the Cerenkov threshold there appears to be some fluorescence. This is not unexpected.

CONCLUSIONS

It is believed that the method described in this paper is equally applicable to the proton, light and medium cosmic ray components. It is interesting to note that at 300 Mev/Nuc, the alpha spectrum is still rising rapidly toward lower energies. It is planned to extend these measurements to higher latitudes in the near future.

ACKNOWLEDGEMENTS

The author wishes to express his appreciation to the Office of Naval Research and to Winzen Research of Minneapolis, Minnesota, for the excellent balloon services that were provided, and to Dr. J. A. Van Allen for discussing this work critically and offering many valuable comments.

FIGURE CAPTIONS

Fig. 1. Plot of Cerenkov Pulse Height in 1" Lucite radiator vs the most probable energy loss for protons and alphas in a 1/8" Na-I crystal. Fast albedo particles will be along A-B. R-B represnets particles below geomagnetic cut-off. Triangles represent observed response of Cerenkov detector to fast multiply charged particles in Flight III.

Fig. 2. Schematic Drawing of Telescope.

Fig. 3. Schematic Diagram of electronic circuits.

Fig. 4. - 0 - Experimental pulse height distribution for sea level mu mesons. Dashed line is calculated curve for Williams-Landau distribution.

Fig. 5. Calculated Williams-Landau Distribution for alpha particles of 1.5, .8, .4, .3 and .2 Bev Nucleons. P (E) represents probability of energy loss E in crystal by a particle of given energy.

Fig. 6. Comparison of alpha pulse height distribution (- 0 -) in ionization detector (Flt. I, $\lambda = 41^{\circ}$) with sea level mu meson distribution. (Both curves normalized to same area).

Fig. 7. Experimental sea level Mu meson pulse height distribution in Cerenkov detector. Dashed line represents Poisson distribution with $\bar{n} = 34$.

Fig. 8. Time altitude curve for Flt. I (San Angelo, Texas, 17 January 1955) and Flt. III (Minneapolis, Minn., 7 July 1955).

Fig. 9. Raw Differential Pulse Height Data in α region. Ionization intervals have been selected so that there is, to a crude approximation, equal number of α counts/interval in the energy sensitive region. The ordinate scale represents the actual numbers of counts at altitude.

Fig. 10. Differential pulse height data of Figure 9. Heavy dashed line represented background counts in interval. ---Δ--- gives distribution of J counts in interval.

Fig. 11. Vertical intensity of alpha particles as a function of atmospheric depth. This gives an apparent mean free path of 45 ± 7 gms as indicated by solid line.

Fig. 12. Plot of Kinetic Energy/Nucleon as a function of the most probable energy loss in the crystal for α particles.

Fig. 13. Differential Energy spectrum for primary alphas. The emulsion data obtained by Waddington[10] is shown for comparison. The data has been fitted to a curve of the form $J\ (\ = E) = \frac{c}{(1+E)^{\gamma}}$. The point on the right at 1.3 Bev was obtained

using data at $\lambda = 41^{\circ}$. This is only point involving geomagnetic theory and was disregarded in fitting the data.

Fig. 14. Integral energy spectrum of primary alpha particles. Point at 1.7 Bev/ nucleon based on $\lambda = 41^{\circ}$ data.

Fig. 15. Observed hourly rates for total alpha, fast alpha ($E >$ 800 Mev/nucleon) slow alpha ($E <$ 800 Mev/Nucleon) and total telescope rate. Time is Central Standard Time.

Fig. 16. Plot of Cerenkov light in kinetic energy/ nucleon for alpha particles. Experimental points have been normalized to theoretical curve at highest experimental point.

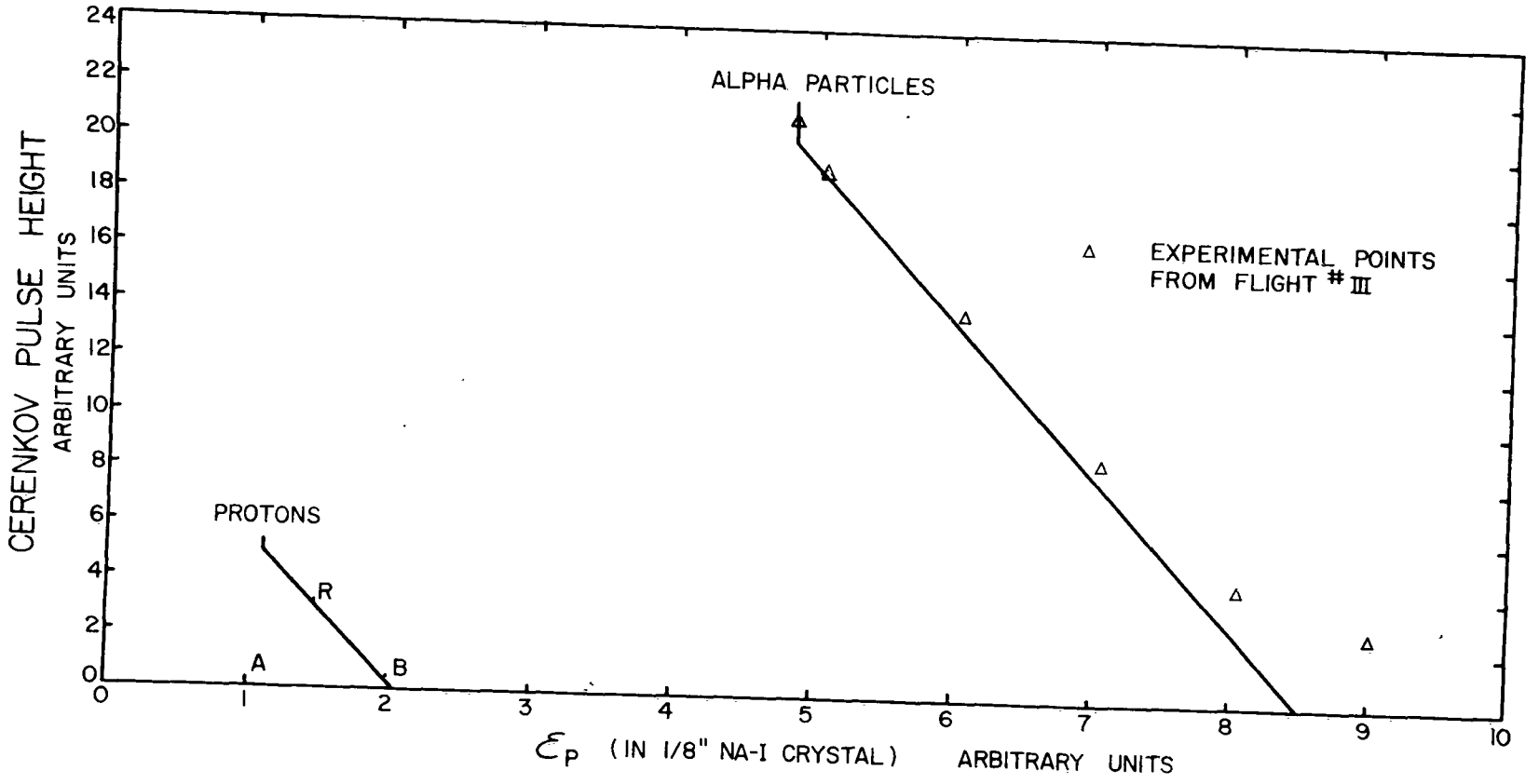
CERENKOV PULSE HEIGHT
ARBITRARY UNITS
ALPHA PARTICLES
EXPERIMENTAL POINTS
FROM FLIGHT # III
PROTONS
R
A
B
$\mathcal{E}_P$ (IN 1/8" NA-I CRYSTAL) ARBITRARY UNITS

FIG. 1

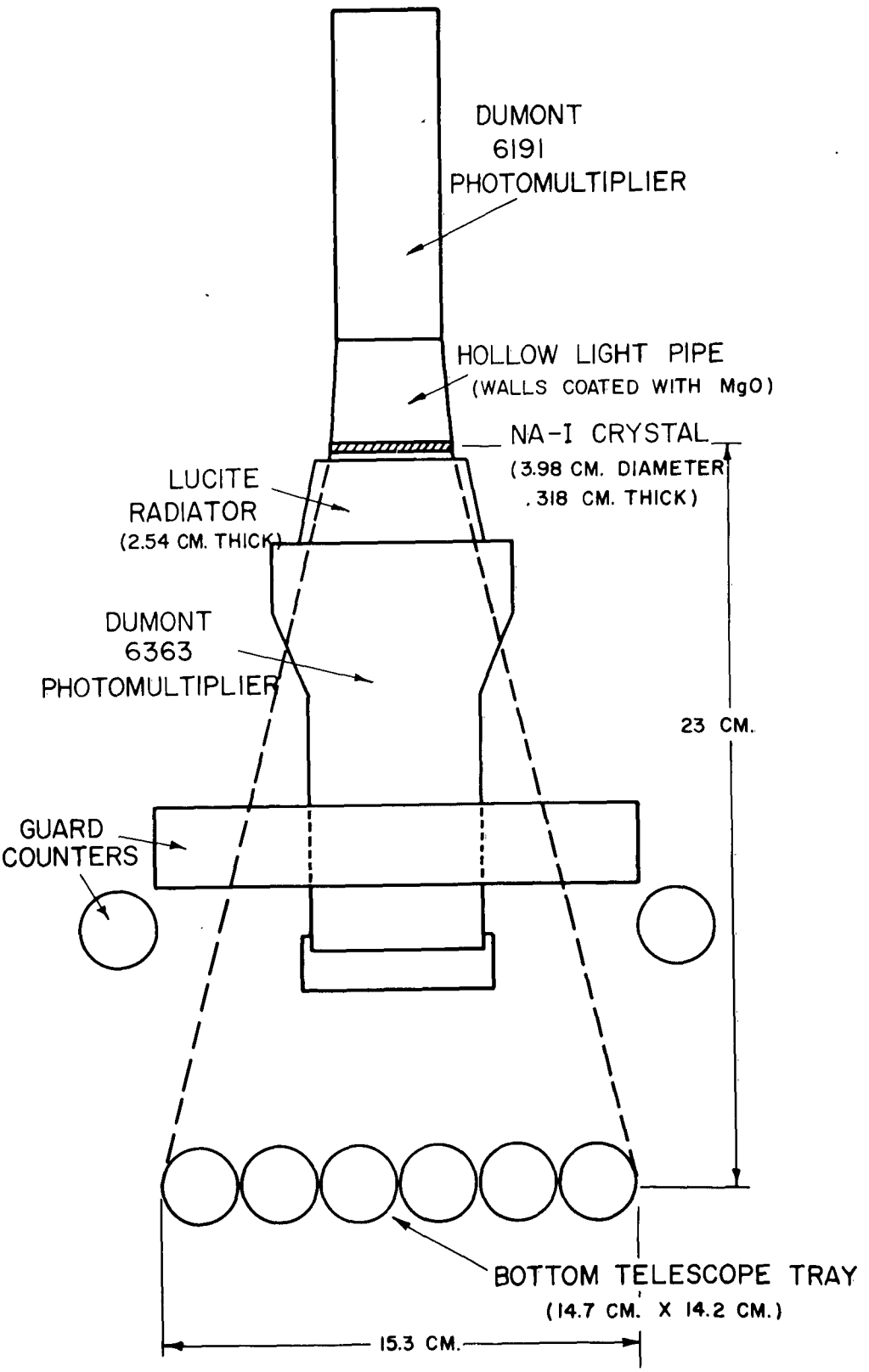
DUMONT
6191
PHOTOMULTIPLIER
HOLLOW LIGHT PIPE
(WALLS COATED WITH MgO)
NA-I CRYSTAL
(3.98 CM. DIAMETER
.318 CM. THICK)
LUCITE
RADIATOR
(2.54 CM. THICK)
DUMONT
6363
PHOTOMULTIPLIER
23 CM.
GUARD
COUNTERS
BOTTOM TELESCOPE TRAY
(14.7 CM. X 14.2 CM.)
15.3 CM.

FIG. 2

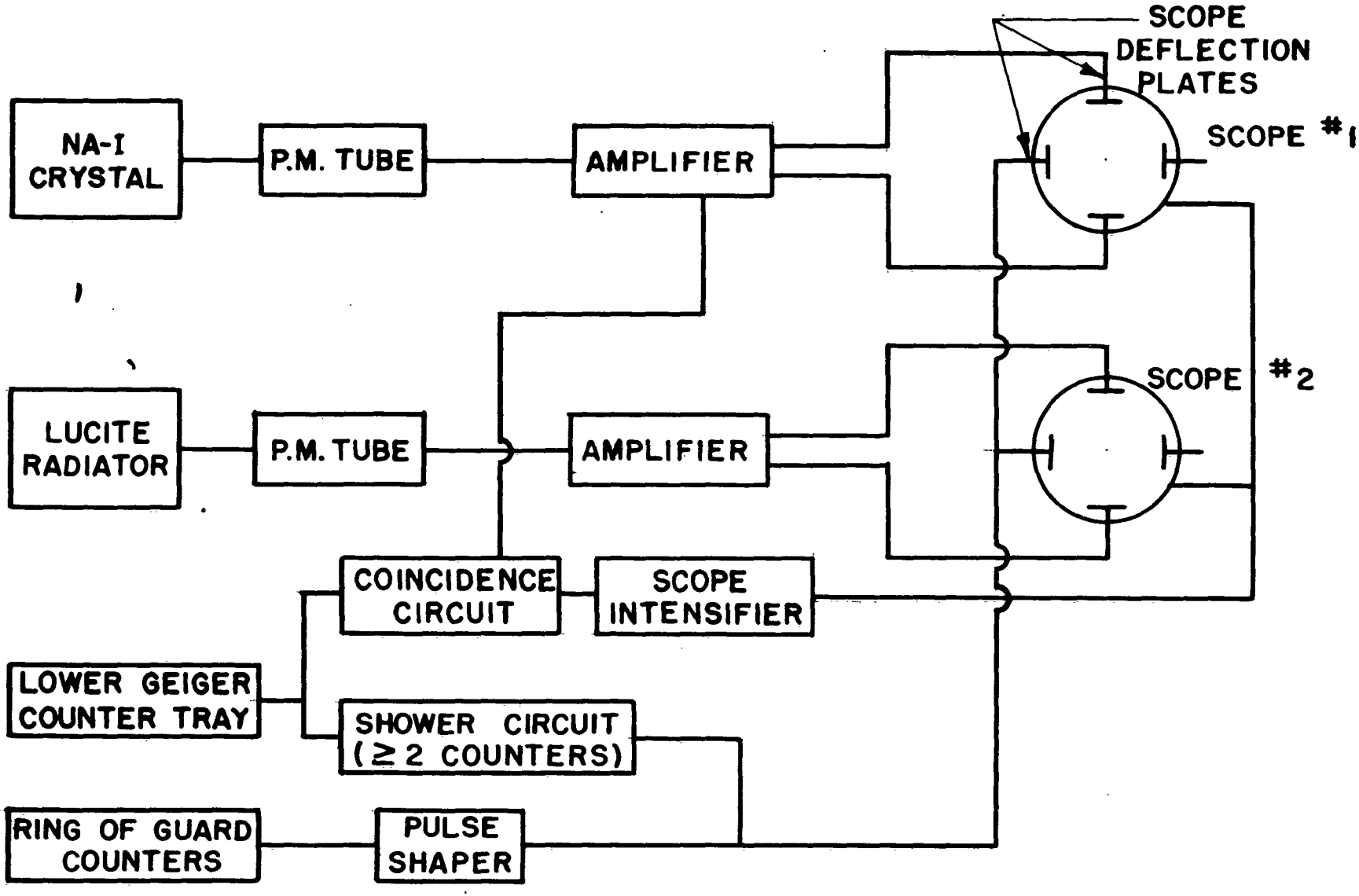
NA-I CRYSTAL
P.M. TUBE
AMPLIFIER
SCOPE DEFLECTION PLATES
SCOPE #1
LUCITE RADIATOR
P.M. TUBE
AMPLIFIER
SCOPE #2
COINCIDENCE CIRCUIT
SCOPE INTENSIFIER
LOWER GEIGER COUNTER TRAY
SHOWER CIRCUIT (≥2 COUNTERS)
RING OF GUARD COUNTERS
PULSE SHAPER

FIG. 3

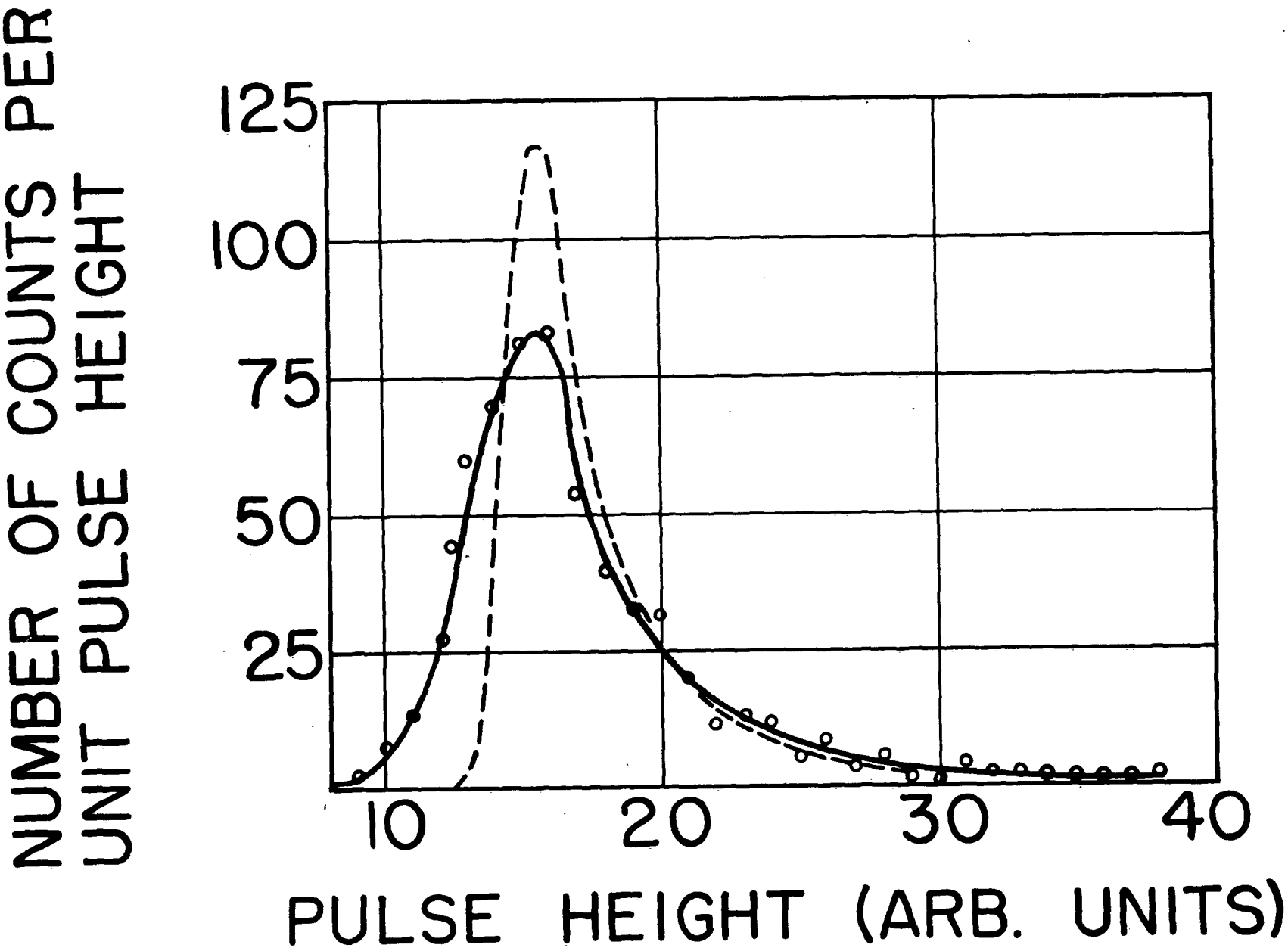
NUMBER OF COUNTS PER UNIT PULSE HEIGHT
125
100
75
50
25
10
20
30
40
PULSE HEIGHT (ARB. UNITS)

FIG. 4

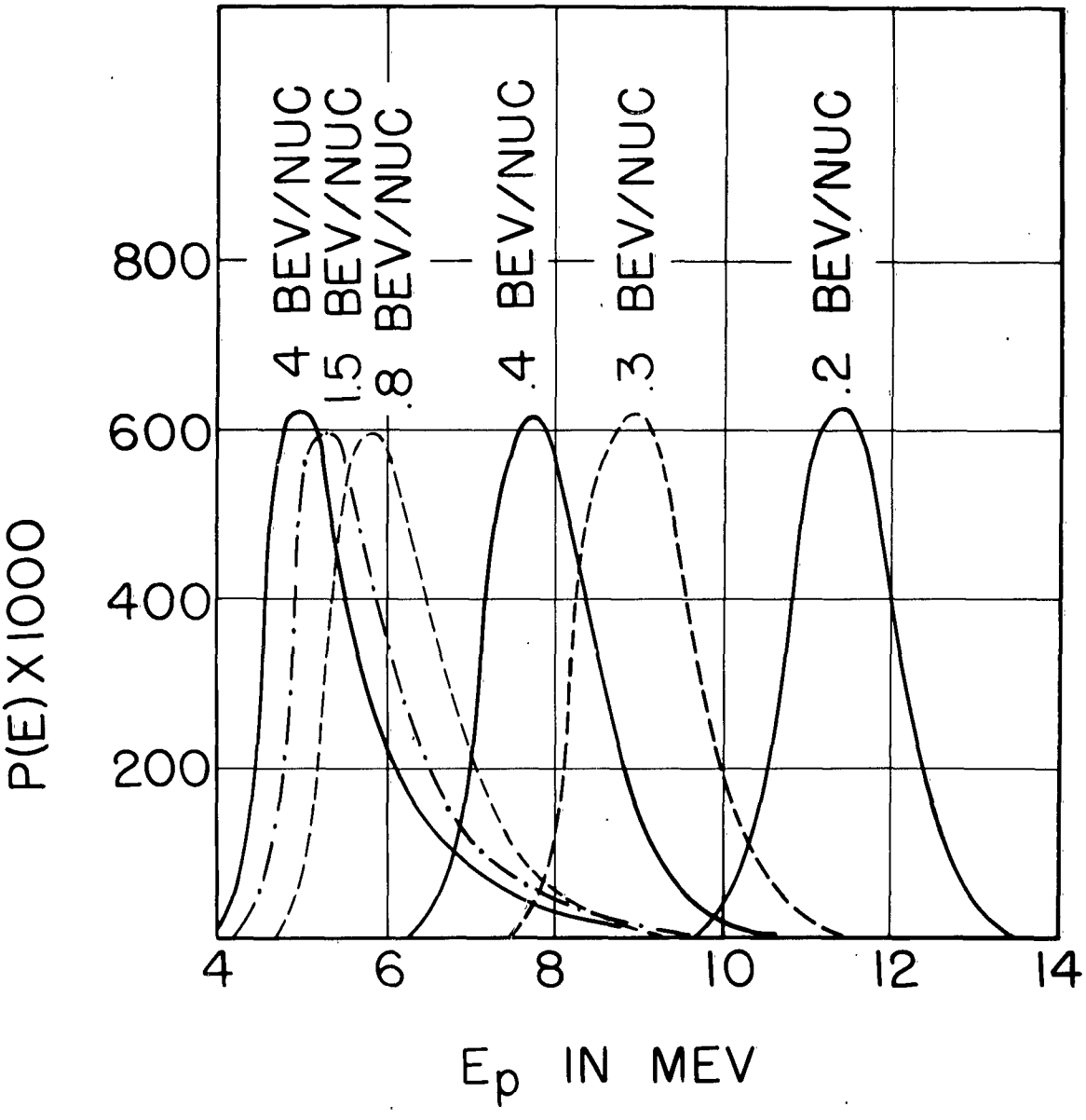
4 BEV/NUC
1.5 BEV/NUC
.8 BEV/NUC
.4 BEV/NUC
.3 BEV/NUC
.2 BEV/NUC
800
600
400
200
P(E) X 1000
4
6
8
10
12
14
Ep IN MEV

FIG. 5

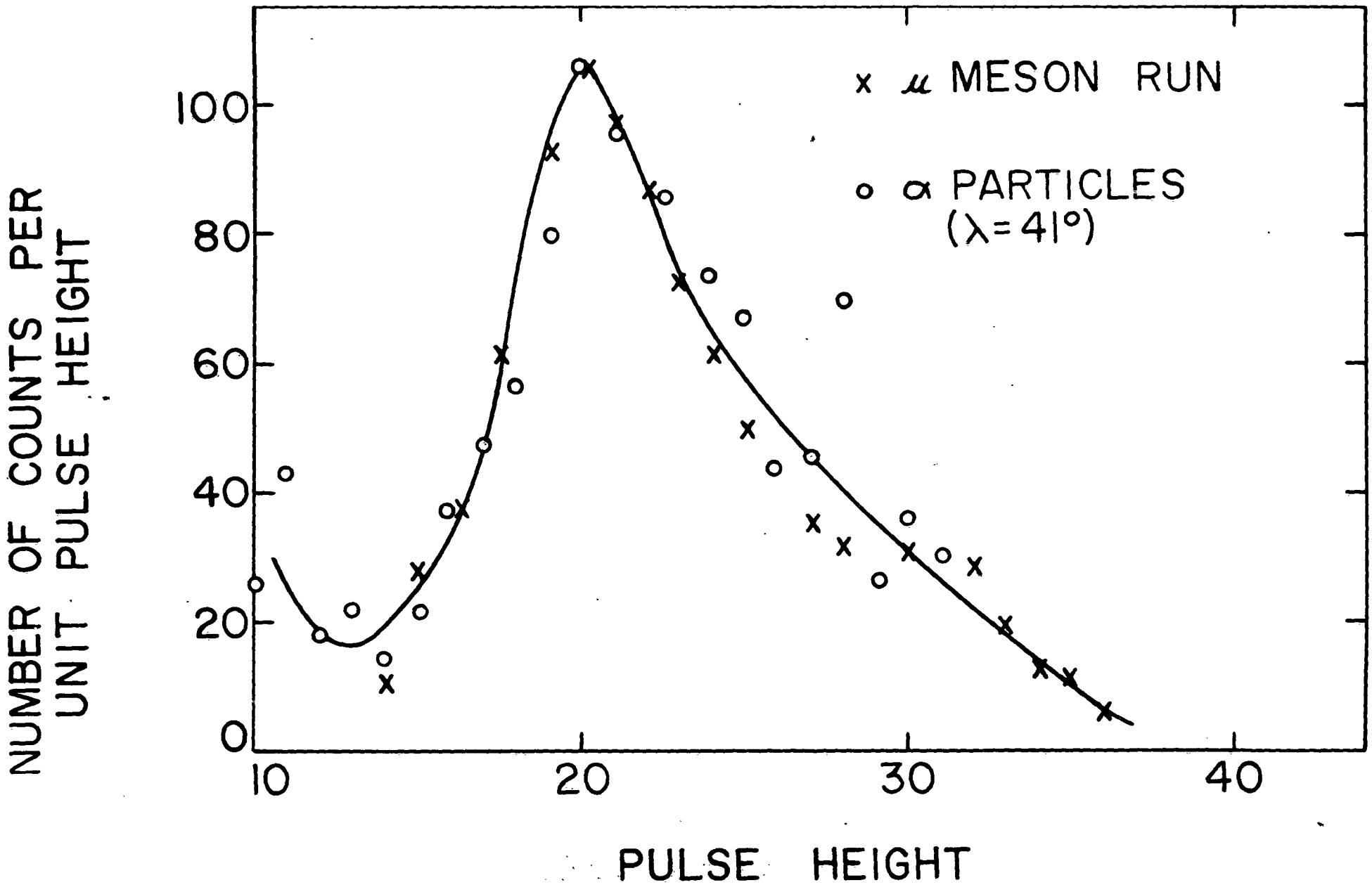
NUMBER OF COUNTS PER UNIT PULSE HEIGHT
100
80
60
40
20
0
10
20
30
40
PULSE HEIGHT
x μ MESON RUN
o α PARTICLES
(λ=41°)

FIG. 6

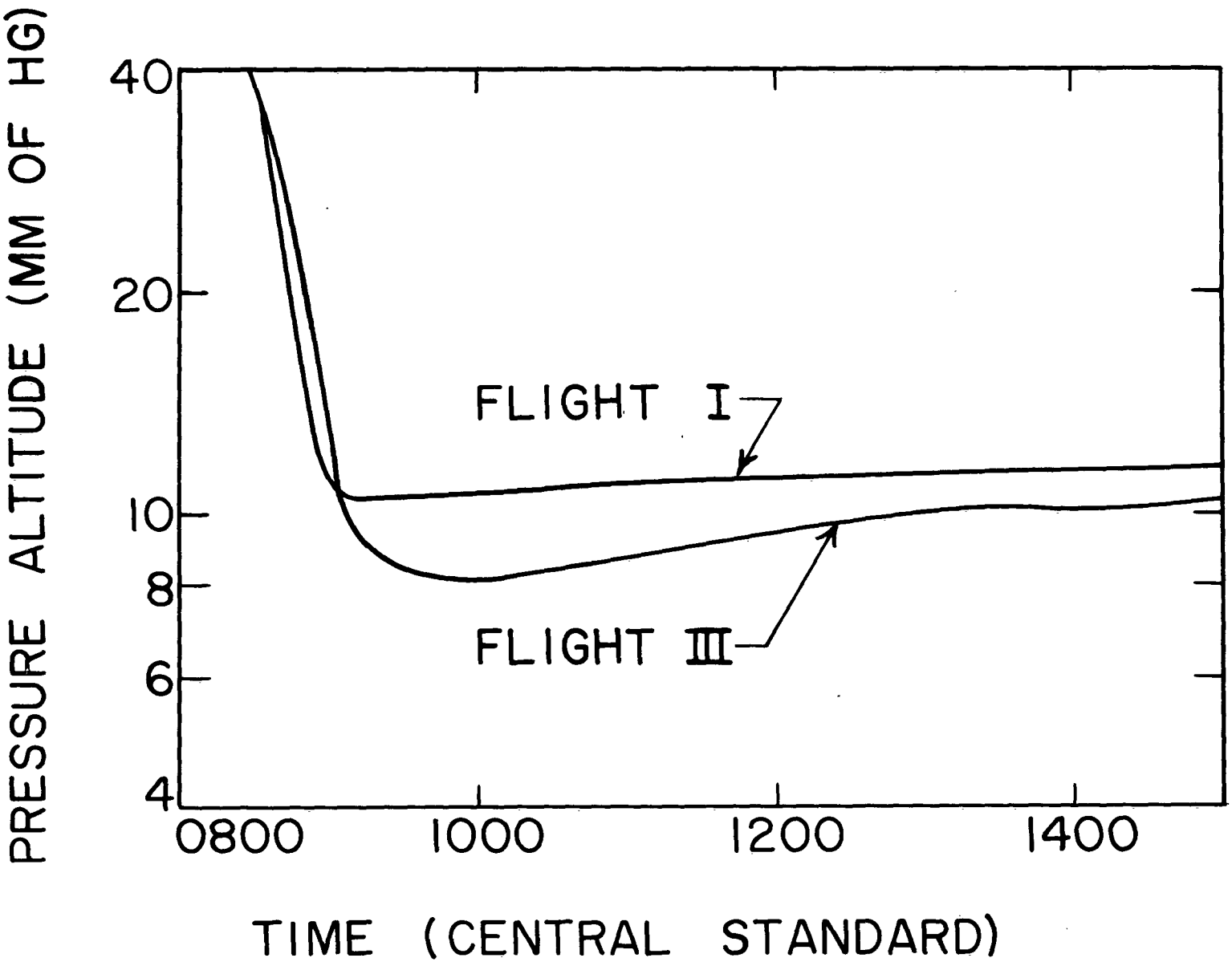
PRESSURE ALTITUDE (MM OF HG)
40
20
10
8
6
4
FLIGHT I
FLIGHT III
0800
1000
1200
1400
TIME (CENTRAL STANDARD)

FIG. 8

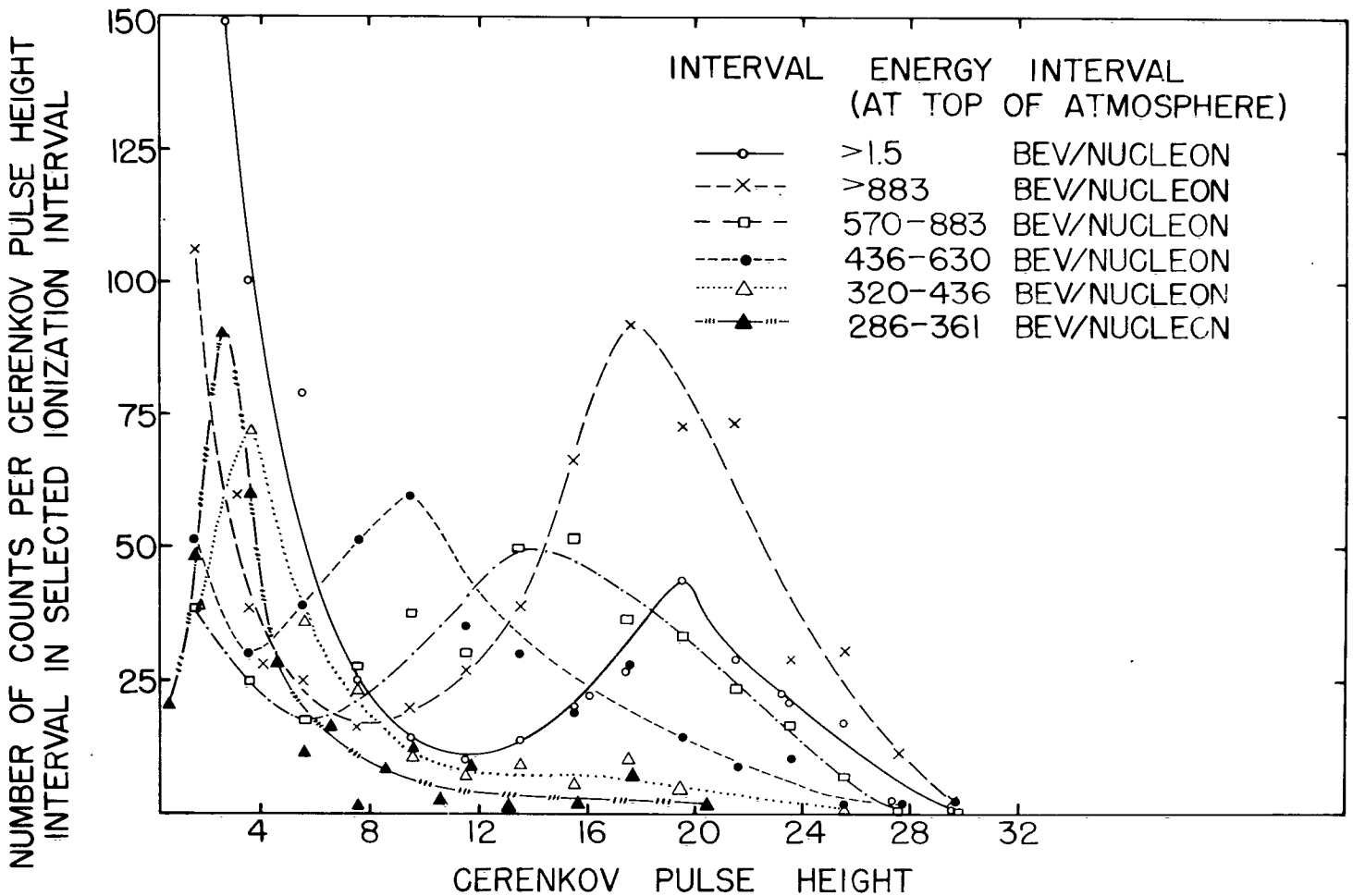
NUMBER OF COUNTS PER CERENKOV PULSE HEIGHT INTERVAL IN SELECTED IONIZATION INTERVAL
150
125
100
75
50
25
4
8
12
16
20
24
28
32
CERENKOV PULSE HEIGHT
INTERVAL ENERGY INTERVAL (AT TOP OF ATMOSPHERE)
>1.5 BEV/NUCLEON
>883 BEV/NUCLEON
570-883 BEV/NUCLEON
436-630 BEV/NUCLEON
320-436 BEV/NUCLEON
286-361 BEV/NUCLECN

FIG. 9

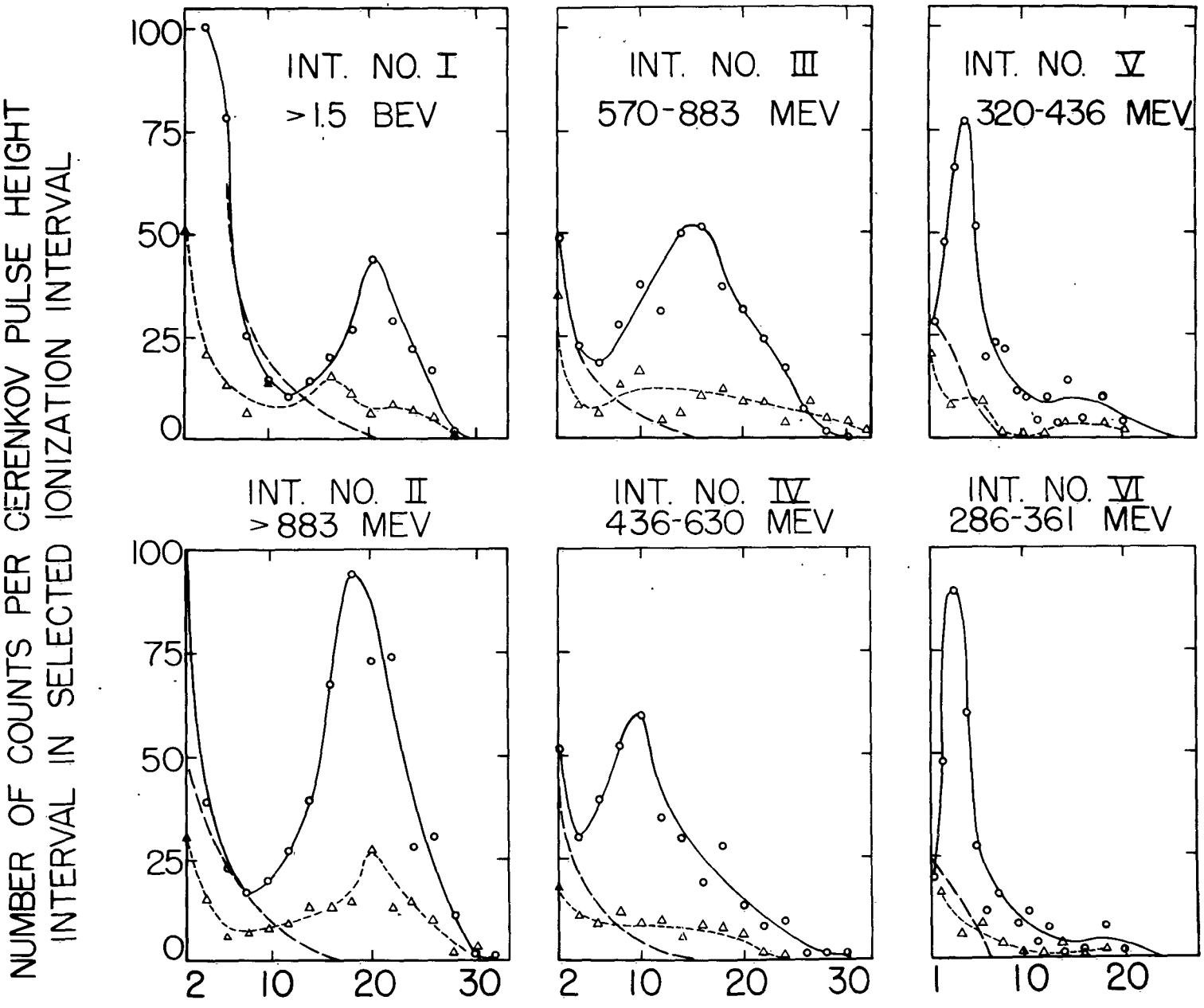
NUMBER OF COUNTS PER CERENKOV PULSE HEIGHT INTERVAL IN SELECTED IONIZATION INTERVAL
INT. NO. I
>1.5 BEV
INT. NO. III
570-883 MEV
INT. NO. V
320-436 MEV
INT. NO. II
>883 MEV
INT. NO. IV
436-630 MEV
INT. NO. VI
286-361 MEV
100
75
50
25
0
2
10
20
30
1
CERENKOV PULSE HEIGHT

FIG. 10

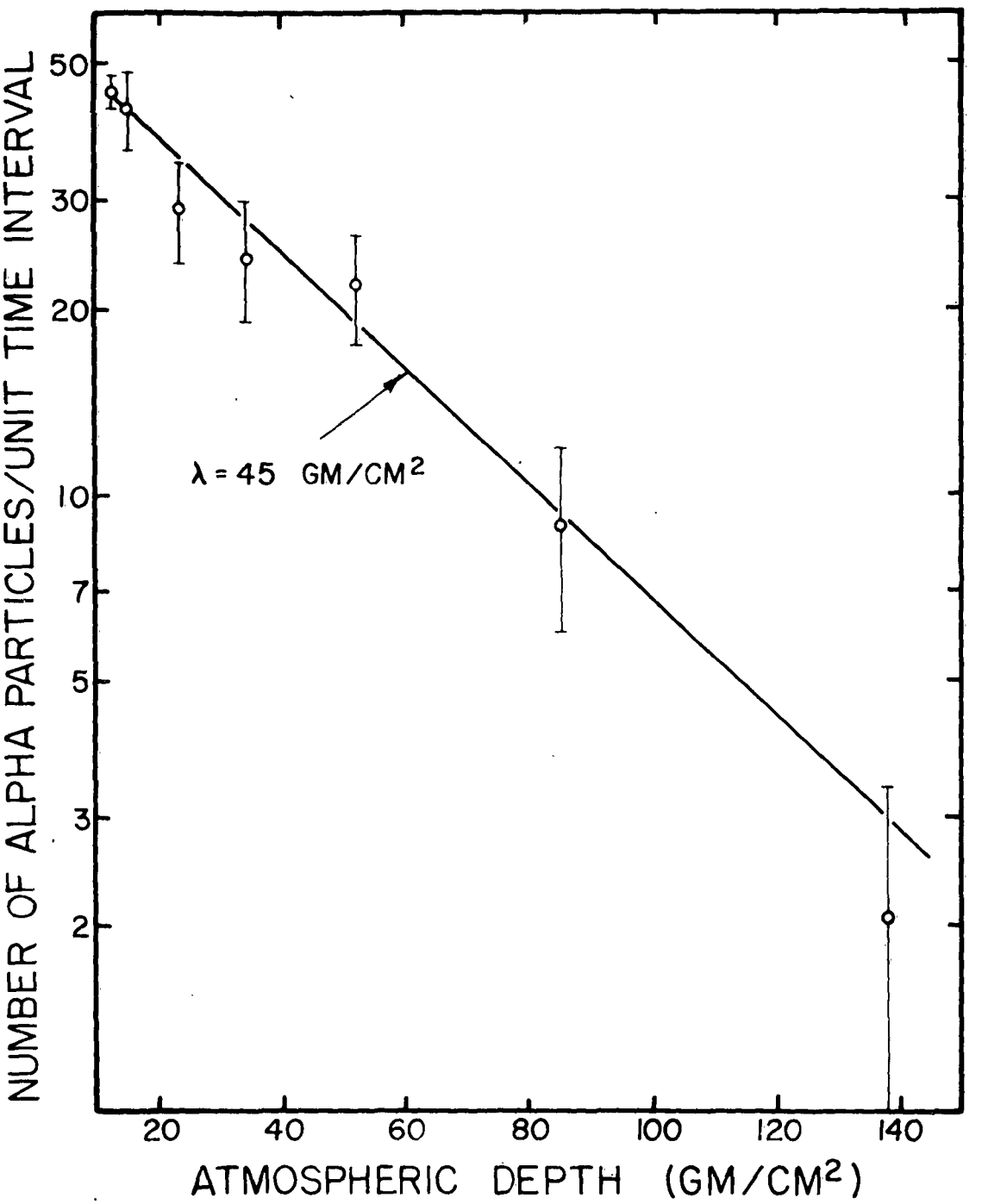
NUMBER OF ALPHA PARTICLES/UNIT TIME INTERVAL
50
30
20
10
7
5
3
2
λ = 45 GM/CM²
20
40
60
80
100
120
140
ATMOSPHERIC DEPTH (GM/CM²)

FIG. 11

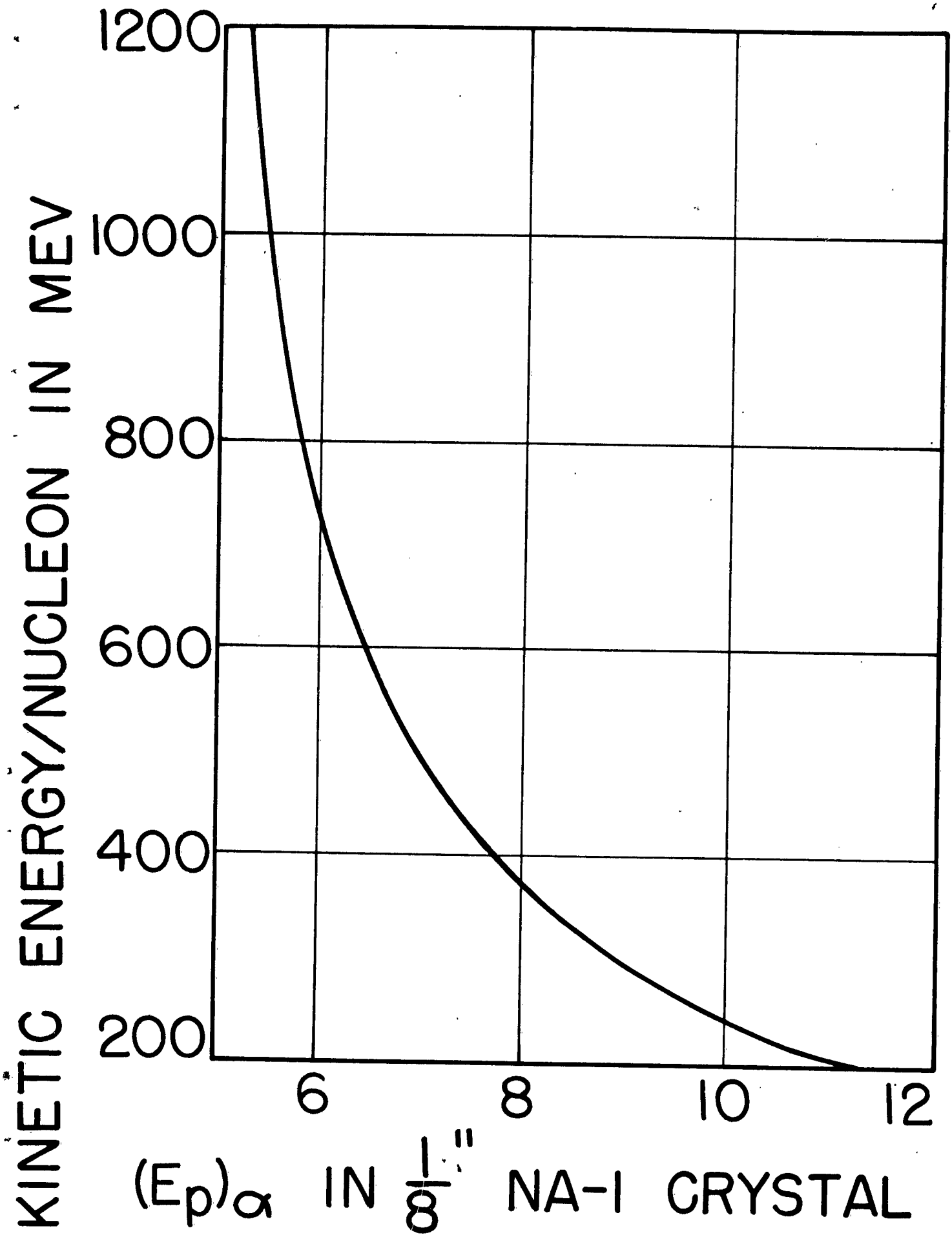
KINETIC ENERGY/NUCLEON IN MEV
1200
1000
800
600
400
200
6
8
10
12
$(E_p)_\alpha$ IN $\frac{1}{8}$" NA-I CRYSTAL

FIG. 12

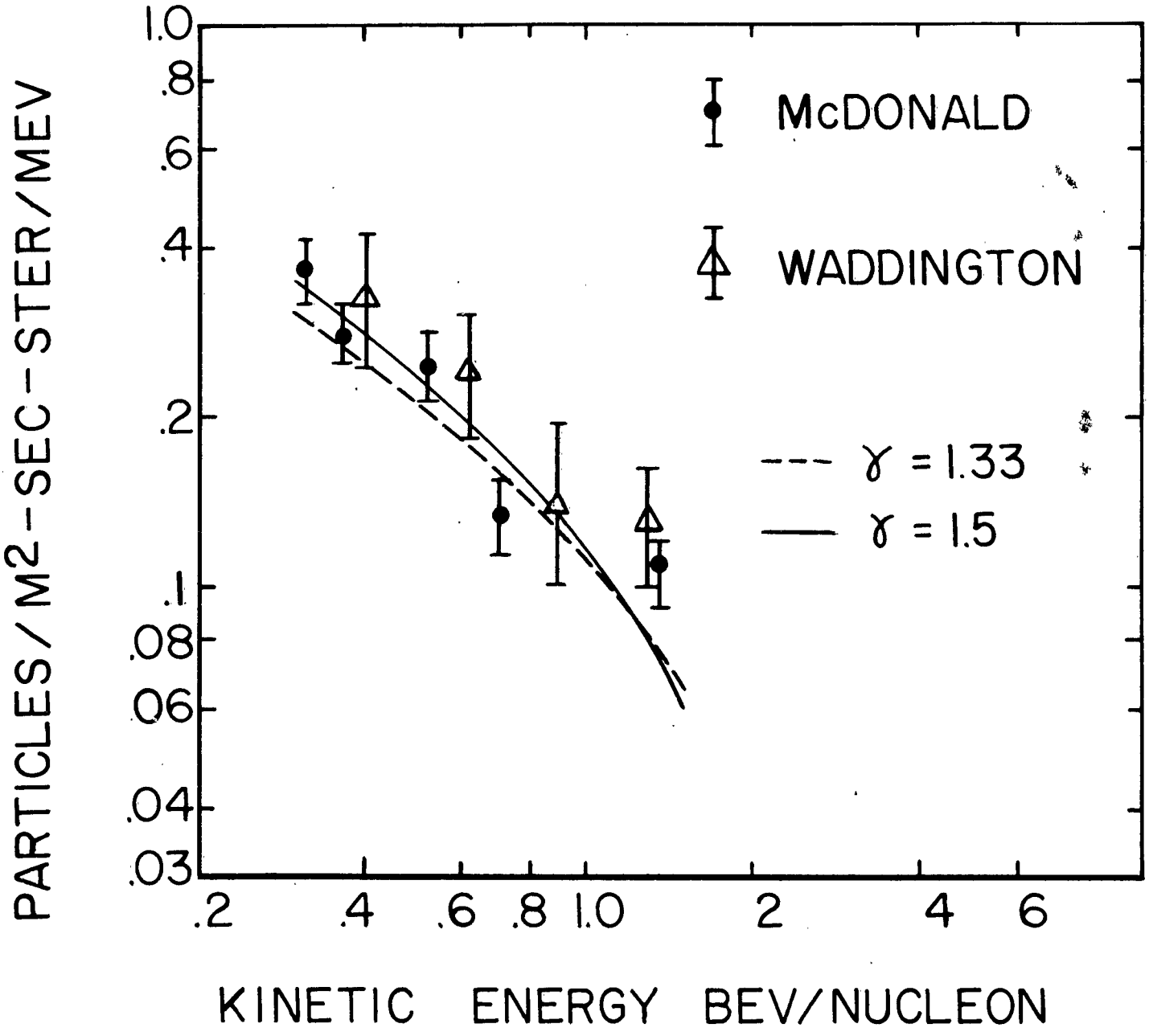
PARTICLES / M2 - SEC - STER / MEV
1.0
.8
.6
.4
.2
.1
.08
.06
.04
.03
.2
.4
.6
.8
1.0
2
4
6
KINETIC ENERGY BEV/NUCLEON
McDONALD
WADDINGTON
--- γ = 1.33
—— γ = 1.5

FIG. 13

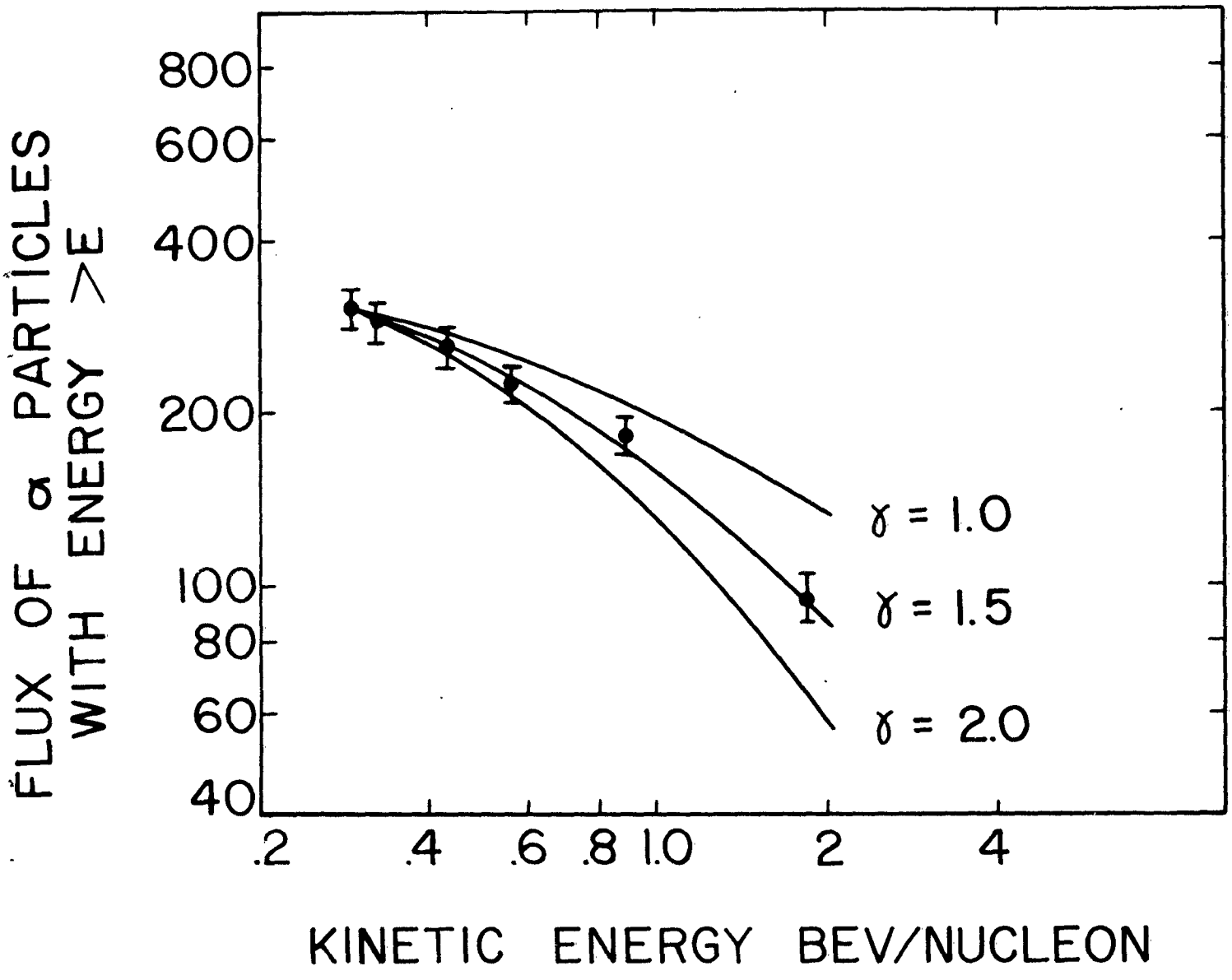
FLUX OF α PARTICLES WITH ENERGY >E
800
600
400
200
100
80
60
40
.2
.4
.6
.8
1.0
2
4
γ = 1.0
γ = 1.5
γ = 2.0
KINETIC ENERGY BEV/NUCLEON

FIG. 14

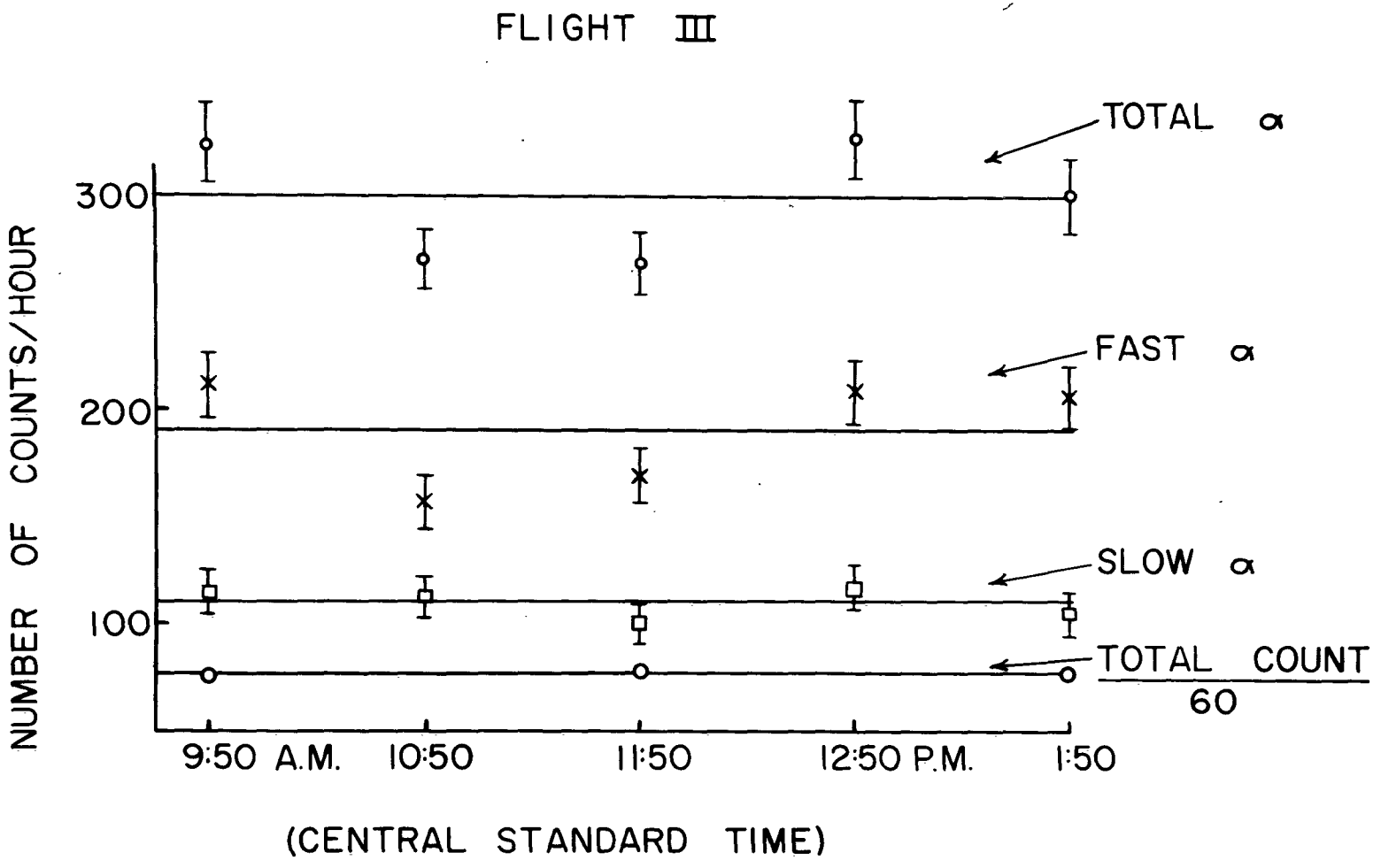
FLIGHT III
TOTAL α
FAST α
SLOW α
TOTAL COUNT / 60
300
200
100
NUMBER OF COUNTS/HOUR
9:50 A.M.
10:50
11:50
12:50 P.M.
1:50
(CENTRAL STANDARD TIME)

FIG. 15

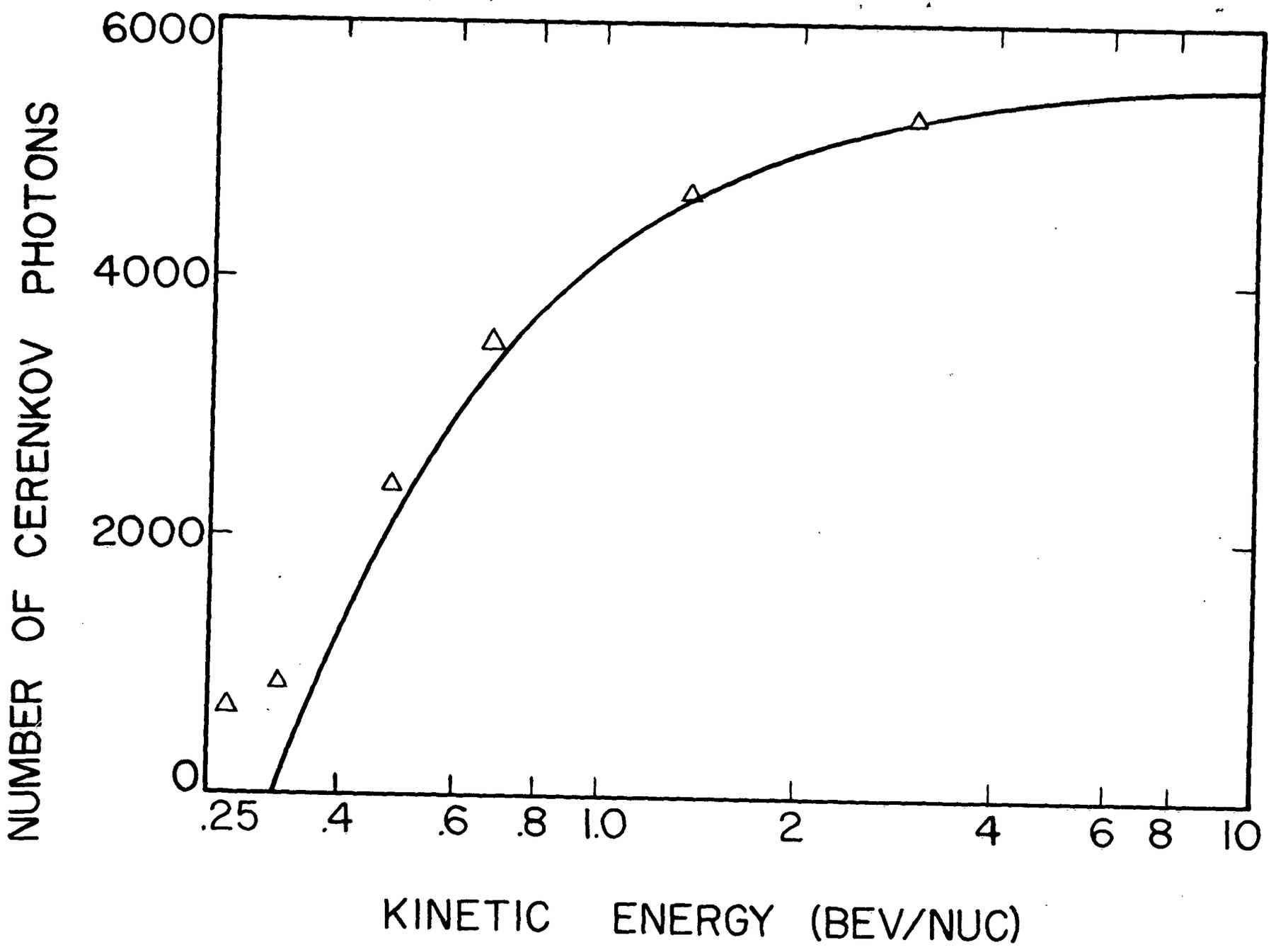
6000
4000
2000
0
NUMBER OF CERENKOV PHOTONS
.25
.4
.6
.8
1.0
2
4
6
8
10
KINETIC ENERGY (BEV/NUC)

FIG. 16